

Stability and Change in Perception: Spatial Organization in Temporal Context

Sergei Gepshtein
University of California at Berkeley

Michael Kubovy
University of Virginia

Keywords:

VISION, PERCEPTUAL ORGANIZATION, MULTISTABILITY, ADAPTATION, HYSTERESIS, BIAS, ORIENTATION-TUNING, SENSORY INTEGRATION

We presented observers with two successive multistable stimuli and found that the higher the probability of the favored organization in the first stimulus the lower the probability of the same organization in the second. This pattern of negative contingency is orientation-tuned and occurs no matter whether the favored organization had or had not been experienced in the first stimulus. The effect of negative contingency combines multiplicatively with another effect that *increases* the likelihood of the just-perceived organization. Both effects can be explained without assuming either adaptation or hysteresis in perceptual organization. Our data suggest that the observed effects reveal lasting states of the visual system rather than changes in the system caused by stimulation.

We usually perceive a stable visual world with no hint of ambiguity of visual stimulation. But because such ambiguity exists the brain must often make perceptual decisions: it must select among the perceptual alternatives that are consistent with the optical stimulation (Helmholtz, 1867/1962; Ittelson, 1952; Rock, 1975; Marr, 1982). Normally, these decisions are hidden from awareness; they are “unobservable” (or “private”). One way to make the process of perceptual selection observable is to look at ambiguous—or “multistable”—figures (Julesz & Chang, 1976; Kruse & Stadler, 1995; Kanizsa & Luccio, 1995).

Thanks to studies of animals viewing multistable figures (reviewed in Leopold & Logothetis, 1999 and Blake & Logothetis, 2002) we understand some of the mechanisms responsible for perceptual selection. Several interpretations of a multistable stimulus are represented in the visual cortical activity concurrently, even though only one of the alternatives is perceived at a time. How can perceptual experience be stable and continuous in the presence of other interpretations? To answer this question, we must understand the interplay of two counteracting temporal tendencies in the perception of multistable figures: *hysteresis* and *adaptation*. Hysteresis increases the likelihood of the current percept in the next

instant; adaptation decreases it:

Hysteresis. This tendency resembles a memory-like phenomenon in a system whose state depends on its history. If the perception of an ambiguous stimulus persists even after the stimulus has been changed to the point where its geometry favors an alternative interpretation, the perceptual system is said to show hysteresis with respect to this type of ambiguous stimulus (Fender & Julesz, 1967; Williams, Phillips, & Sekuler, 1986; Hock, Kelso, & Schöner, 1993; Kruse & Stadler, 1995).

Adaptation. This tendency resembles the common perceptual process in which prolonged exposure to a stimulus makes the system less sensitive to the parameters of the stimulus (e.g., Hochberg, 1950; Kruse, Stadler, & Wehner, 1986). Following Köhler and Wallach (1944) and Carlson (1953), a common explanation of the reduced sensitivity is neural fatigue (reviewed in Rock, 1975, pp. 265-270; but see Barlow, 1990 for a different explanation).

Because these two tendencies oppose each other, they may cancel out and obscure their individual contributions and the rules of their combination. In this study we describe a method that allows us to separate the two effects and determine how they combine.

Our method is a development of the technique introduced by Hock, Schöner, and Hochstein (1996), who used bistable motion quartets (Schiller, 1933; Figure 1). These are apparent motion displays that allow two interpretations, which in Figure 1 are horizontal motion and vertical motion. Motion is seen more often between dots separated by the shorter spatial distance. Let d_h and d_v stand for horizontal and vertical inter-dot distances, respectively. By manipulating the aspect

We are grateful to H. Hock and D. R. Proffitt for valuable discussions, and to W. Epstein, H. Hock and J. Wagemans for helpful suggestions about an early version of the manuscript. This work was supported by NEI Grant R01 EY 12926. Send correspondence to either author at 360 Minor Hall, Vision Science, University of California at Berkeley, Berkeley, CA 94720-2020, U.S.A., sergeg@uclink.berkeley.edu (S.G.) or Department of Psychology, University of Virginia, P.O. Box 400400, Charlottesville, VA 22904-4400, U.S.A., kubovy@virginia.edu (M.K.).

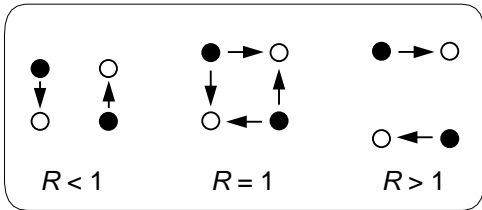


Figure 1. Motion quartets. Two pairs of identical dots (shown here as filled and open circles) are presented in alternation in the opposite corners of a rectangle. When the quartet aspect ratio R is equal to one, perception readily alternates between the two directions of motion—vertical and horizontal. The likelihood of these two percepts varies with R .

ratio, $R = d_v/d_h$, one can vary the probabilities of the two alternative motion directions, as shown in Figure 1.

Hock et al. showed observers two motion quartets— M_1 (*adapting*) and M_2 (*test*)¹—in rapid succession in order to discover whether the visual system is adapted by the unperceived interpretations of M_1 . They manipulated the aspect ratio R_1 of quartet M_1 , and kept the aspect ratio of M_2 constant and unbiased: $R_2 = 1.0$. They obtained the probabilities of the observers’ responses to M_1 and M_2 and asked how R_1 affects the perception of M_2 rather than asking how the *perception* of M_1 (m_1), affects the perception of M_2 (m_2). This question dictated the design of the experiment: They considered only those trials in which *vertical* motion was perceived during the adapting phase, $m_1 = \downarrow$. (In other words, the authors held the observer’s percept of M_1 constant.) The dependent variable was the probability of *horizontal* motion during the test phase, $p(m_2) = \leftrightarrow$. The results were clear. They found that the conditional probability of reporting $m_2 = \leftrightarrow$ after seeing $m_1 = \downarrow$, $p(m_2 = \leftrightarrow | m_1 = \downarrow)$ was a decreasing function of R_1 . They interpreted their results as evidence of adaptation of the visual system by a representation of M_1 that was not experienced but whose existence left a trace in the system that affected the perception of M_2 : They reasoned that increasing R_1 led to a greater strength of the (unperceived) representation of horizontal motion, which in turn caused a greater adaptation to horizontal motion and reduced the likelihood of this motion in M_2 .

We too study perceptual selection, but we use static rather than dynamic multistable stimuli. We generalize the method of Hock et al. such that we can also measure percept-percept correlations. This allows us to observe the balance between the counteracting trends in perception of multistable figures; we find that their effects combine multiplicatively. We also find that the interactions between successive perceptual organizations are orientation-tuned. The results suggest a hypothesis that does not require adaptation and hysteresis as causal factors in perceptual selection. According to this hypothesis, the temporal contingencies between successive perceptual organizations occur because of lasting states of the visual system and not because the preceding stimulus changes (e.g., adapts) the system such as to affect the perception of succeeding stimuli.

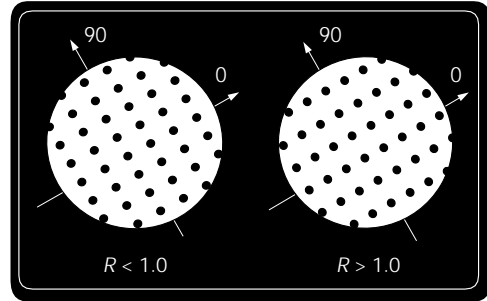


Figure 2. Two rectangular dot lattices in the rotating system of Cartesian coordinates (not to scale). **Left** When the aspect ratio is $R = d_{90}/d_0 < 1.0$ we tend to see the lattice organized parallel to 90° (notated as $l \rightarrow 90$). **Right** When the aspect ratio is $R > 1.0$ we tend to see it organized parallel to 0° ($l \rightarrow 0$).

Experiment 1

In this experiment, we presented observers with a succession of two multistable dot lattices— L_1 and L_2 —and recorded their perception of each lattice.

Method

Observers. Five observers participated in Experiment 1: one of the authors and four undergraduate students who did not know the purpose of the experiment. All the observers had normal or corrected-to-normal vision.

Stimuli. Our L_1 stimuli were *rectangular* dot lattices (Figure 2). (For the nomenclature of dot lattices, see Kubovy, 1994.) The lattices were presented at random orientations by aligning one of the principal organizations of L_1 with an axis of a randomly-oriented system of Cartesian coordinates, whose origin was at the center of a circular aperture (as shown in Figure 2). We will refer to this axis as 0° . Observers are most likely to see such a lattice as a collection of strips parallel to 0° or 90° . (The randomly chosen 0° orientation was the same for both successive lattices.)

The organization of L_1 is controlled by its aspect ratio $R_1 = d_{90}/d_0$, where d_0 and d_{90} represent the inter-dot distances along the orientations parallel to 0° and 90° , respectively (Figure 2). We will notate the percept of a lattice L_i parallel to an orientation ξ° as

$$l_i \rightarrow \xi.$$

For example, we will write the two most likely percepts of L_1 as $l_1 \rightarrow 0$ and $l_1 \rightarrow 90$.

Our L_2 stimuli were *hexagonal* dot lattices (Figure 3), for which the three most likely perceptual organizations were parallel to 0° , 60° and 120° . These percepts are approximately equiprobable and exhaustive, i.e., $p(l_2 \rightarrow 0) \approx p(l_2 \rightarrow 60) \approx p(l_2 \rightarrow 120) \approx 1/3$. We used hexagonal lattices as L_2 because they are the most unstable dot lattices (Kubovy &

¹We describe the experiments of Hock et al. (1996) using a convention different from theirs.

Wagemans, 1995) and are therefore most sensitive to imbalances in the mechanisms underlying perceptual grouping.

Dot diameter in L_1 , L_2 , and the mask was 0.16 degrees of visual angle (dva). At $R_1 = 1.0$, the inter-dot distance was about 1 dva. To preserve the scale of lattices with other values of R_1 , the inter-dot distances were computed so that their product, $d_0 \times d_{90}$, was invariant. For example, with $R_1 = 1.3$ the inter-dot distances were: $d_0 = 0.88$ dva and $d_{90} = 1.14$ dva.

Procedure. Each trial consisted of six successive screens (Figure 3): fixation, lattices L_1 and L_2 , two response screens (one to report l_1 , the other to report l_2) and mask. Four of these—fixation, L_1 , L_2 and mask—were presented on the background of a white circular aperture in a black field, subtending 11.5 dva. The fixation consisted of a dot in the center of the aperture. The mask consisted of a sequence of randomly positioned black dots, whose locations were updated at 60 Hz.

On each trial, lattices L_1 and L_2 were aligned with the 0° axis, which was randomly oriented (with 1° resolution) to minimize the propagation of perceptual bias between the trials.

Observers were asked to report the perceptual organization of L_1 and L_2 by clicking on icons in the corresponding successive response screens. Each response screen consisted of four icons, each containing a line parallel to one of the possible organizations in the corresponding dot lattice (Figure 3).

Each observer contributed 120 trials to each of the five values of R_1 .

Results

We plot the results on a logit scale, where

$$\text{logit}[p(l_1 \rightarrow 0)] = \ln \frac{p(l_1 \rightarrow 0)}{p(l_1 \rightarrow 90)}, \quad (1)$$

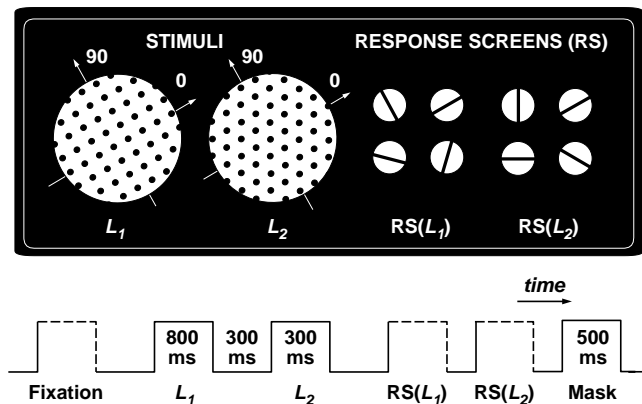


Figure 3. **Top panel** The two successive lattices—rectangular L_1 and hexagonal L_2 —and the two corresponding response screens. The fixation mark and the mask are not shown. **Bottom panel** The trial time line. The dashed segments represent durations under the observer's control.

and

$$\text{logit}[p(l_2 \rightarrow 0)] = \ln \frac{p(l_2 \rightarrow 0)}{\frac{p(l_2 \rightarrow 60) + p(l_2 \rightarrow 120)}{2}}. \quad (2)$$

We averaged the data across observers and then computed $\text{logit}[p(l_1 \rightarrow 0)]$ to overcome floor effects at high aspect ratios.

In the responses to L_1 , we found that $\text{logit}[p(l_1 \rightarrow 0)]$ increases as a linear function of R_1 (Figure 4A). These results replicate the results in previous studies of perceptual grouping (e.g., Kubovy, Holcombe, & Wagemans, 1998) and thus serve as a control.

In the following description of Experiment 1, and in Results of Experiment 2, we adopt the common convention in which persistence of a percept is described as “hysteresis.” We will refer to the negative contingency between the successive percepts as a function of R_1 as “effect of R_1 .”

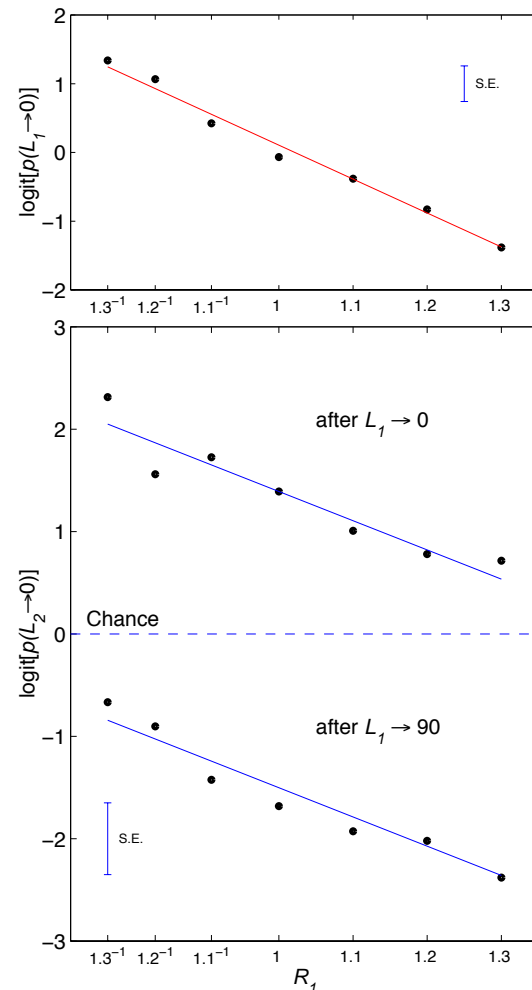


Figure 4. Results of Experiment 1. **A** Responses to L_1 . The data are well described by a linear model ($R^2 = 0.987$). **B** Responses to L_2 , conditionalized by the percepts of L_1 . The label “after $l_1 \rightarrow 0$ ” refers to events [$l_2 \rightarrow 0 | l_1 \rightarrow 0$]. The label “after $l_1 \rightarrow 90$ ” refers to events [$l_2 \rightarrow 0 | l_1 \rightarrow 90$]. The variability in the two sets of data is well explained by a linear model (multiple regression $R^2 = 0.985$).

To study the effect of perception of L_1 on the perception of L_2 , we separate the trials on which $l_1 \rightarrow 0$ responses occurred from trials on which $l_1 \rightarrow 90$ responses occurred. By doing so we isolate the effect of perceptual hysteresis. Because hysteresis is a tendency to perceive the same organization in L_2 as in L_1 , we expect to find a higher likelihood of $l_2 \rightarrow 90$ after $l_1 \rightarrow 90$ than after $l_1 \rightarrow 0$. Indeed, we find that $p(l_2 \rightarrow 90|l_1 \rightarrow 90)$ is above chance and $p(l_2 \rightarrow 0|l_1 \rightarrow 90)$ is below chance for all values of R_1 (Figure 4B). Thus, by computing the conditional probabilities $p(l_2 \rightarrow 0|l_1 \rightarrow 0)$ and $p(l_2 \rightarrow 0|l_1 \rightarrow 90)$, we obtain one set of observations affected by hysteresis and another not affected by it. The results in Figure 4B show a clear segregation between the two sets of data, which are well described by two parallel linear functions. The vertical separation between the two functions is a measure of perceptual hysteresis.

Besides the effect of hysteresis we observe an effect of R_1 . Both $p(l_2 \rightarrow 0|l_1 \rightarrow 0)$ and $p(l_2 \rightarrow 0|l_1 \rightarrow 90)$ decrease as a function of R_1 . Because R_1 controls the perceptual organization of L_1 , this effect could be summarized as follows: The higher the likelihood of a particular organization in L_1 the lower is the likelihood of the same organization in L_2 . Similar effects were interpreted in the literature as evidence of adaptation in multistable figures (reviewed in Hock et al., 1996). The effect of R_1 on $p(l_2 \rightarrow 0|l_1 \rightarrow 90)$ corresponds to what Hock et al. called “adaptation to an unperceived organization of L_1 ,” consistent with the notion that the visual system registers several organizations of a multistable stimulus, even though only one of them reaches awareness at a time.

The observation that the two sets of data are well described by two parallel linear functions implies that the effects of R_1 and hysteresis on $\logit[p(l_2 \rightarrow 0)]$ are additive, confirming the independence of the two effects. This additivity in logit space means that the effects of these variables on $p(l_2 \rightarrow 0)$ are multiplicative: the effect of R_1 over its domain is to decrease $p(l_2 \rightarrow 0)$ by a factor of 4.6; the effect of hysteresis increases $p(l_2 \rightarrow 0)$ by a factor of 18.1.

Experiment 2

In this experiment we rotated L_2 with respect to L_1 to find a range of angular alignment between L_1 and L_2 for which the correlations between the percepts of the two stimuli still hold.

Method

In this experiment we used square (rather than hexagonal) lattices as L_2 and rotated them with respect to L_1 by an angle θ ($0^\circ \leq \theta \leq 45^\circ$), in four steps of 15° . In square lattices, the inter-dot distances along 0° and 90° are equal and the corresponding most likely percepts are equiprobable and equally misaligned with the rectangular L_1 lattice. The angle $\theta = 45^\circ$ was a control condition, in which $l_2 \rightarrow 0$ is equidistant from the adapting orientations of 0° and 90° . The duration of L_1 was 500 ms. Three observers participated in this experiment. None of the observers knew the purpose of the experiment. The experiment was otherwise identical to Experiment 1.

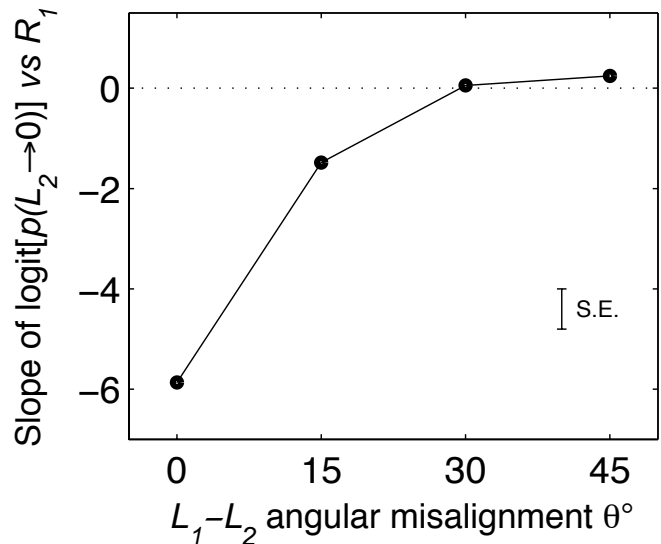


Figure 6. Summary of Experiment 2. The negative slopes in Figure 5 vanish as the angular misalignment θ between L_1 and L_2 approaches 30° .

Results

We averaged the values of $\logit[p(l_1 \rightarrow 0)]$, which were computed separately for each observer. The results are shown in Figure 5. Although in this experiment we used a square lattice rather than a hexagonal one as L_2 , at the misalignment of $\theta = 0^\circ$ the results are similar to what we observed in the first experiment: We find clear effects of both R_1 and hysteresis on the perception of L_2 . As expected, both effects disappear in the control condition of $\theta = 45^\circ$, indicated by the lack of vertical separation between the data sets $p(l_2 \rightarrow 0|l_1 \rightarrow 0)$ and $p(l_2 \rightarrow 0|l_1 \rightarrow 90)$, and the lack of a negative slope in the fitting functions.

The effects of R_1 and hysteresis behave differently as a function of θ . As we increase θ , the slopes of both functions $p(l_2 \rightarrow 0|l_1 \rightarrow 0)$ and $p(l_2 \rightarrow 0|l_1 \rightarrow 90)$ rapidly drops to zero. We summarize this results in Figure 6 by plotting the average slope of the two functions against θ . Evidently, the effect of R_1 is substantially reduced (by a factor of 4) as θ grows from 0° to as small a misalignment as 15° . The effect of R_1 disappears completely at $\theta = 30^\circ$. On the contrary, the effect of hysteresis is still evident at $\theta = 30^\circ$, although it is reduced by a factor of 6, as compared to its maximal value at $\theta = 0^\circ$.

Discussion

We presented observers with two successive dot lattices— L_1 and L_2 —and manipulated the aspect ratio of L_1 . We found two contingencies between the perception of successive stimuli: (1) observers preferred to see the same organization in L_1 and L_2 , but (2) increasing the likelihood of an organization in L_1 decreased the likelihood of seeing the same organization in L_2 , whether or not that organization was experienced in

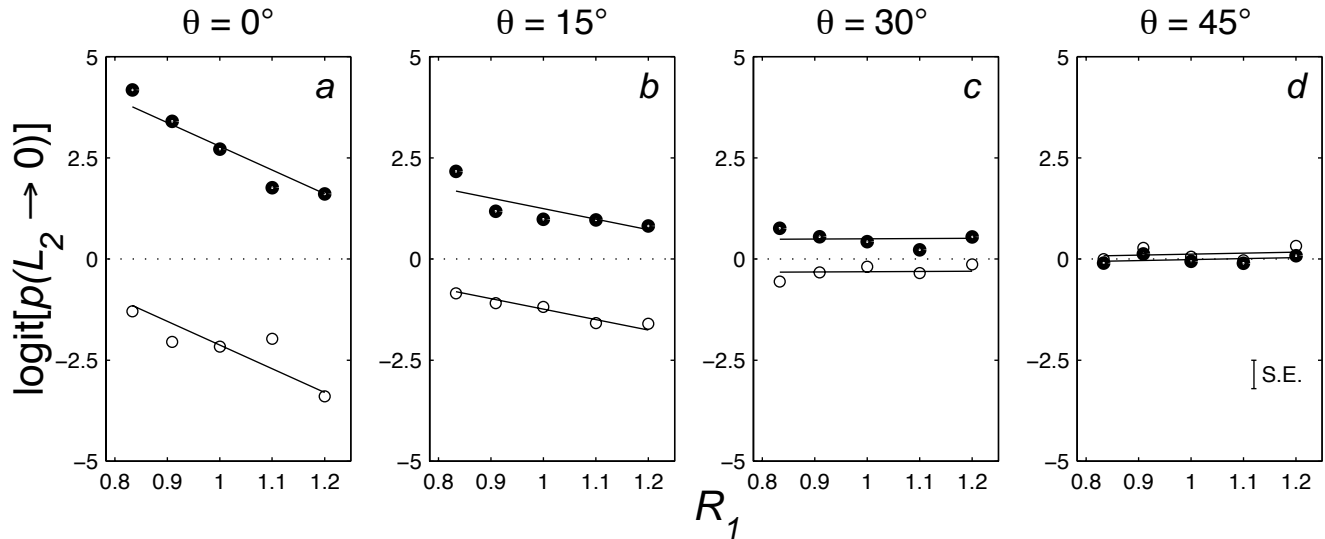


Figure 5. Results of Experiment 2. **A-D** Plots for the four values of orientation misalignment (θ) between L_1 and L_2 . Each plot uses the format of Figure 4B, where θ was equal to 0° .

L_1 .

Observers' preference for the same perceptual organization is a manifestation of perceptual persistence that is often called hysteresis. The second effect is the negative contingency between the likelihood (strength) of a potential percept in the preceding stimulus and the likelihood of seeing the same organization in the succeeding stimulus. Similar negative contingency has been attributed to sensory adaptation (Hock et al., 1996). Adopting the above view of perceptual selection, we could summarize our results as follows. We showed that unperceived interpretations of static perceptual groupings cause selective orientation-tuned adaptation just as they did in multistable apparent motion. Beyond that, we also measured the contribution of perceptual hysteresis and found that the effects of adaptation and hysteresis are independent and combine multiplicatively.

As we show below, however, our results also agree with a different hypothesis that explains the contingencies between perception of successive multistable figures without invoking mechanisms such as hysteresis or adaptation. Next, we elaborate the hypothesis and then illustrate it using a probabilistic model.

Hypothesis of persistent bias

Repetitive changes in the perception of unchanging multistable figures reveal a factor of perceptual organization which is intrinsic to the brain and which alters perception in an apparently random fashion (Borsellino et al., 1972; Ditzinger & Haken, 1990; Hock, Schöner, & Voss, 1997; Hock, Schöner, & Giese, 2003; Hupé & Rubin, 2003). We will call this factor an *intrinsic bias*. Because of this bias the perception of multistable figures is probabilistic: We know the likelihood of a particular percept but we are not certain whether the percept would occur in a particular trial. By varying stimulus geometry, however, we can change the likelihood of the per-

cept. For example, events $l_1 \rightarrow 0$ are more likely than events $l_1 \rightarrow 90$ when $R_1 > 1$. We will call such contribution of stimulus geometry a *stimulus support* of a particular organization in a multistable figure.

Multistable figures can be perceived in a way inconsistent with stimulus support. For example, event $l_1 \rightarrow 0$ happens with a measurable likelihood when $R_1 < 1$, even though stimulus support favors $l_1 \rightarrow 90$. Presumably, such events come about when intrinsic bias happens to exceed stimulus support. How do the fluctuations of intrinsic bias relative to stimulus support manifest themselves in our results?

Consider, first, those cases where event $l_1 \rightarrow 0$ happened at $R_1 \ll 1$ (Figure 4A), i.e., against the stimulus support of L_1 . In those trials, the intrinsic bias that favored $l_1 \rightarrow 0$ was presumably greater than the stimulus support. Notice also that after event $l_1 \rightarrow 0$ at $R_1 \ll 1$, we found a high likelihood of event $l_2 \rightarrow 0$ (top left in Figure 4B). That is to say, observers were likely to see L_2 organized parallel to 0° after they say L_1 organized parallel to 0° against the stimulus support of L_1 . It seems plausible that the same intrinsic bias that overcame stimulus support in favor of 0° in L_1 , also tipped the balance in favor of 0° in L_2 , whose geometry was equally consistent with both 0° and 90° interpretations.

When $R_1 \gg 1$, however, events $l_1 \rightarrow 0$ occur in agreement with the stimulus support of L_1 , so that the data in the right part of the top function in Figure 4B do not correspond to only those trials where intrinsic bias supported 0° . Consistent with this observation, we found that here function $p(l_2 \rightarrow 0 | l_1 \rightarrow 0)$ drops toward the chance level, as one would expect from the neutral configuration of L_2 (recall that $R_2 = 1$).

Thus both the elevation of the left end of function $p(L_2 \rightarrow 0 | l_1 \rightarrow 0)$ (which we previously attributed to hysteresis) and the proximity of its right end to the chance level (which we previously attributed to adaptation), can be explained using

the basic notion of intrinsic bias alone. Similarly, the low likelihood of $l_2 \rightarrow 0$ after $l_1 \rightarrow 90$ at $R_1 > 1$ (the right end of the bottom function in Figure 4B), and the closure of $p(l_2 \rightarrow 0 | l_1 \rightarrow 90)$ to chance level at $R_1 < 1$ can also be explained using the hypothesis of intrinsic bias alone. The only constraint that this hypothesis puts on the properties of intrinsic bias is that at the successive instants of L_1 and L_2 the biases must be similar. We will refer to this idea as *hypothesis of persistent bias*.

Next we test the hypothesis of persistent bias by formulating it explicitly, as a probabilistic model. In a simulation of the model below we examine whether the hypothesis of persistent bias alone can explain both effects observed in Figure 4B.

Model of Persistent Bias

We formulated the model as a sequence of trials (or iterations), each simulating successive presentations of lattices L_1 and L_2 . Each iteration of our simulation proceeded through the following steps:

1. Stimulus support. We computed the attraction strength $s_i^{\mathbf{v}}$ for each potential direction \mathbf{v} (where $\mathbf{v} \in \{\mathbf{b}, \mathbf{c}, \mathbf{d}\}$) in the dot lattices L_i (where $i = 1, 2$), using the Pure Distance Model of grouping by proximity of Kubovy et al. (1998)

$$s_i^{\mathbf{v}} = e^{-\alpha \left(\frac{|\mathbf{v}|}{|\mathbf{a}|} - 1 \right)}, \quad (3)$$

where α is the *attraction constant*, $|\mathbf{v}|$ is the inter-dot distance in the direction of organization \mathbf{v} , and $|\mathbf{a}|$ is the inter-dot distance of the organization $L_1 \rightarrow 0$. The Pure Distance Model describes how the attraction strength of a certain organization decays as a function of the corresponding inter-dot distance, normalized by a reference inter-dot distance $|\mathbf{a}|$:

$$s_i^{\mathbf{v}} \begin{cases} > 1 & : & 0 < |\mathbf{v}| < |\mathbf{a}| \\ = 1 & : & |\mathbf{v}| = |\mathbf{a}| \\ < 1 & : & |\mathbf{v}| > |\mathbf{a}|. \end{cases} \quad (4)$$

The attraction constant α , which typically varies across observers between 5 and 10, is an index of an observer's sensitivity to the ratio of proximities between the alternative organizations: The larger attraction constant, the higher observer's sensitivity. (For the simulations summarized in Figure 7, $\alpha = 7$.)

2. Intrinsic bias. In our model, bias is a stimulus-independent distribution supporting perceptual organizations for a range of orientations. The mean β_1 of the bias distribution was drawn from the Uniform distribution on the circle:

$$U_c(\theta) = 2\pi U_1, \quad (5)$$

where U_1 is a uniformly distributed random variable on the line interval $[0, 1]$. The random placement of bias distribution in the beginning of every trial reflects the

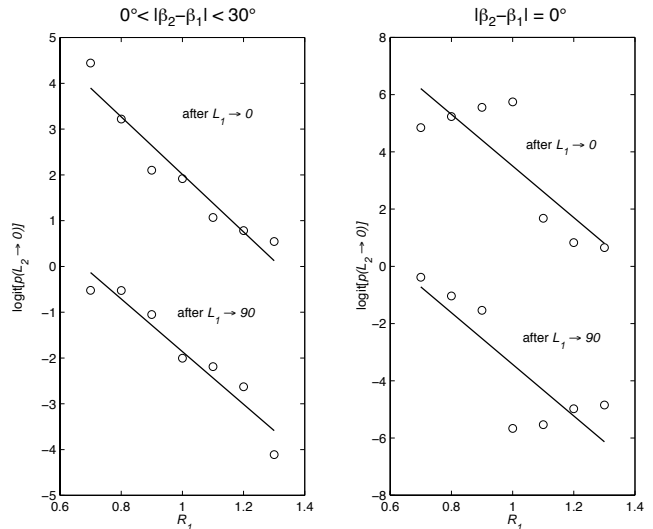


Figure 7. Results of a Monte Carlo simulation of the model of persistent bias with 200 iterations per condition. **A** The simulated data show a “crispening” pattern when the bias distribution does not change across time ($\beta_1 = \beta_2$). **B** The simulation yields a pattern similar to the one observed in the human data (Figure 4B) when the bias is allowed to change (Figure 8).

fact that in our experiments the conditions were randomized across trials, so that any configuration could occur before the current trial. Hence, our method allows us to study contingencies of responses within, and not between, the trials.

We simulated the bias distribution, centered on β_1 , using the Wrapped Cauchy distribution $W(\theta)$, $0 \leq \theta < 2\pi$ (Fisher, 1993, pp. 46–47), which is a computationally efficient approximation to the Gaussian distribution wrapped around the circle. The standard deviation of the distribution was 30° . We computed the weights $w^{\mathbf{v}} \in W(\theta)$ of the bias distribution by drawing values of $W(\theta)$ at the corresponding orientations.

To implement the hypothesis of persistent bias, the mean β_2 of the bias distribution during the presentation of L_2 had to be similar to β_1 . (We will explain how this was achieved in the forthcoming section, “Change of bias across time.”)

3. Decision. Compute the energy $E_i^{\mathbf{v}}$ for each of the four orientations:

$$E_i^{\mathbf{v}} = s_i^{\mathbf{v}} w^{\mathbf{v}} \quad (6)$$

and determine which organization is perceived by choosing the orientation that has the highest energy.

Change of bias across time. The hypothesis of persistent bias holds that the orientation bias in the L_2 phase of each iteration is identical or similar to the bias in the L_1 phase. To implement this idea, we either chose $\beta_2 = \beta_1$ or allowed β_2 to slightly drift away from β_1 . It turns out that this difference causes a significant change in simulation outcomes.

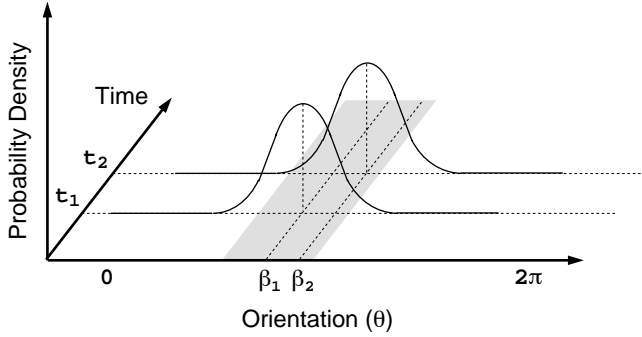


Figure 8. Change in the distribution of intrinsic bias across time, shown on the line rather than on the circle for simplicity. At time t_1 the bias is centered on β_1 . At time t_2 it is centered on β_2 , drawn from a uniform distribution on a narrow interval of θ (shadowed area) whose mean is β_1 .

If $\beta_2 = \beta_1$ (i.e., if the bias distribution does not change during the interval between L_1 and L_2) the data show a “crispening pattern,” evident in Figure 7A:

$$\logit[p(l_2 \rightarrow 0 | l_1 \rightarrow 0)] = f(R_1) \begin{cases} \text{increasing : } R_1 \leq 1 \\ \text{decreasing : } R_1 > 1. \end{cases} \quad (7)$$

Similarly,

$$\logit[p(l_2 \rightarrow 0 | l_1 \rightarrow 90)] = f(R_1) \begin{cases} \text{increasing : } R_1 \geq 1 \\ \text{decreasing : } R_1 < 1. \end{cases} \quad (8)$$

(We explain the causes of “crispening” in the next section.) When, however, the mean of the intrinsic bias distribution changes over time ($\beta_2 \neq \beta_1$), the model yields results similar to human data (Figure 7B).

In the simulation that generated the results shown in Figure 7B, we implemented the change of bias by drawing β_2 from a narrow uniform probability distribution centered on β_1 (Figure 8). Except for its mean β_2 , this distribution was identical to the one we used in the L_1 phase. The results shown in Figure 7B were obtained with the range of U_b equal to the standard deviation of the bias distribution (30°). As the range of U_b grows, the negative slopes of the two functions in Figure 7B approach zero (not shown in the figure). Increasing the range of U_b is equivalent to rotating L_2 relative to L_1 , because in both cases the bias is tuned to 0° in the L_1 phase of a trial will not systematically affect the organization of L_2 . This observation implies that the hypothesis of persistent bias is also consistent with our findings in Experiment 2, that increasing the angular misalignment of L_1 and L_2 brings L_2 out of the effective range of the orientation-tuned bias.

The causes of “crispening”. We found that if the simulated intrinsic bias does not change between the successive stimuli, the model yields a “crispening pattern” (Figure 7A) that is not observed in the human data (Figure 4B). To clarify the causes of “crispening” we plot the simulation results in the format of Figure 9. The figure displays the number of

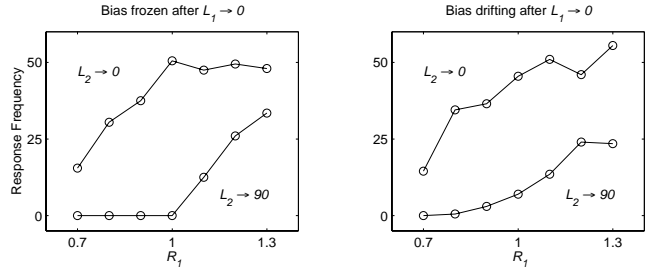


Figure 9. The frequencies of events $l_2 \rightarrow 0$ and $l_2 \rightarrow 90$ after L_1 has been organized parallel to 0° . **A** The bias distribution was identical in the L_1 and L_2 phases of each trial. **B** The bias distribution was allowed to slightly change during the interval between the L_1 and L_2 phases (Figure 8). The results of simulations displayed in **A** and **B** were used to obtain the results shown with filled dots on the top of Figure 4A and B, respectively.

simulated events [$l_2 \rightarrow 0 | l_1 \rightarrow 0$] and [$l_2 \rightarrow 90 | l_1 \rightarrow 0$]. The log-ratio between the two data sets in Figure 9A yields the top function in Figure 7A. This function deviates from the human data when $R_1 \leq 1$. Let us consider the cases of $R_1 = 1$ and $R_1 < 1$ separately.

When $R_1 = 1$, events $l_1 \rightarrow 0$ happen only when the intrinsic bias favors organization parallel to 0° . Thus, when $\beta_1 = \beta_2$ (as in Figure 9A), L_2 is always organized the same way as L_1 . This explains the fact that events [$l_2 \rightarrow 90 | l_1 \rightarrow 0$] never occur when $R_1 = 1$. However, when $\beta_1 \neq \beta_2$ (as in Figure 9B), the intrinsic bias will sometimes support 0° and sometimes 90° in the the L_1 phase, such that L_2 will also be organized sometimes parallel to 0° and sometimes parallel to 90° .

When $R_1 \ll 1$, the stimulus geometry in L_1 does not favor organization parallel to 0° , so that events $l_1 \rightarrow 0$ happen only when the intrinsic bias supports 0° . Thus, when $\beta_1 = \beta_2$, L_2 can only be organized parallel to 0° (Figure 9A). As R_1 grows within $R_1 < 1$, the stimulus support against 0° decreases and events $l_1 \rightarrow 0$ happen more often. When $\beta_1 \neq \beta_2$, L_2 can sometimes be organized parallel to 90° after the bias has caused organization 0° in L_1 and has moved away such as to support organization 90° in L_2 .

A similar analysis applies to the increasing segment of the data set [$l_2 \rightarrow 0 | l_1 \rightarrow 90$] at $R_1 \geq 1$ in Figure 7A.

Probability matching in perception?

What purpose could be served by having a system in which an orientation-bias drifted over time? We can suggest an account by recalling the phenomenon of probability matching (also known as probability learning; e.g., Estes, 1964 and Gallistel, 1990, pp. 351–383). It has been observed that when animals and humans are given the choice between two alternatives, one of which is rewarded more often than the other, they choose each alternative roughly in proportion to the likelihood of reward. This strategy does not maximize payoff. So why would organisms evolve to favor it? Because

it is suboptimal only in a world in which probabilities are stable. If the animal assumed that the world may change and that the resource at the most generous source is more likely to be exhausted, then the strategy according to which it chooses the most likely alternative may turn out to be short-sighted, and may fail in the long run. Similarly, there is good reason to have a perceptual system evolve in such a way that when the environment admits of more than one interpretation, one sometimes favors one, and other times another, even when one of the interpretations is more likely to be correct. Indeed, probability matching occurs in visual behavior (Kowler & Anton, 1987; Triesch, Ballard, & Jacobs, 2002). A drifting orientation bias could be an instantiation of such a perceptual strategy.²

Perceptual multistability may be a special case of the organism's attempt to take into account as much information as possible. Depending on whether the information from different sources is consistent or not, the organism may treat multiple source of information as being antagonistic or synergistic. When the information is consistent, all the sources contribute to the percept (for example, by taking the weighted sum of the corresponding estimates: Landy & Kojima, 2001; Ernst & Banks, 2002; Gepshtein & Banks, 2003; Alais & Burr, 2004, or by being super-additive: Kubovy, Cohen, & Hollier, 1999). When it is inconsistent, synergy fails and the percept is either based on a sub-additive combination of the sources (Kubovy et al., 1999) or on one of the sources at a time (winner-take-all). Because of its probabilistic nature, the latter process is sometimes called *stochastic integration* (Ghahramani, Wolpert, & Jordan, 1997), similar to the aforementioned probability matching.

Multistable figures are designed such that their several interpretations are conspicuously inconsistent with one other. So, it is not surprising that the dynamics of multistability resemble that of stochastic integration. It remains to be seen whether the model of drifting bias, which we have shown to account for the dynamics of multistable figures, can also explain the dynamics of other cases of stochastic integration.

References

- Alais, D., & Burr, D. (2004). The ventriloquist effect results from near-optimal bimodal integration. *Curr Biol*, *14*, 257–262.
- Barlow, H. B. (1990). A theory about the functional role and synaptic mechanism of visual after-effects. In C. Blakemore (Ed.), *Vision: Coding and efficiency* (pp. 363–75). New York: Academic Press.
- Blake, R., & Logothetis, N. K. (2002). Visual competition. *Nat Rev Neurosci*, *3*, 13–21.
- Borsellino, A., Allazetta, A., Bartolini, B., Rinesi, S., & DeMarco, A. (1972). Reversal time distribution in the perception of visual ambiguous stimuli. *Kybernetik*, *10*, 139144.
- Carlson, V. R. (1953). Satiation in a reversible perspective figure. *J Exp Psychol*, *45*, 442–448.
- Carpenter, R. H. S. (1999). A neural mechanism that randomises behavior. *J Consc Studies*, *6*, 13–22.
- Ditzinger, T., & Haken, H. (1990). The impact of fluctuations on the recognition of ambiguous patterns. *Biol Cybern*, *63*, 453–456.
- Ernst, M. O., & Banks, M. S. (2002, January). Humans integrate visual and haptic information in a statistically optimal fashion. *Nature*, *415*(24), 429–433.
- Estes, W. K. (1964). Probability learning. In A. W. Melton (Ed.), *Categories of human learning*. New York: Academic Press.
- Fender, D., & Julesz, B. (1967). Extension of Panum's fusional area in binocularly stabilized vision. *J Opt Soc Am*, *57*, 819–830.
- Fisher, N. I. (1993). *Statistical analysis of circular data*. New York: Cambridge University Press.
- Gallistel, C. R. (1990). *The organization of learning*. Cambridge: The MIT Press.
- Gepshtein, S., & Banks, M. S. (2003). Viewing geometry determines how vision and touch combine in size perception. *Curr Biol*, *13*, 483–488.
- Ghahramani, Z., Wolpert, D. M., & Jordan, M. I. (1997). Computational models of sensorimotor integration. In P. G. Morasso & V. Sanguineti (Eds.), *Self-organization, computational maps and motor control* (pp. 117–147). Elsevier Press.
- Helmholtz, H. von. (1867/1962). *Treatise on physiological optics* (Vol. III. Originally published in 1867). New York: Dover Publications.
- Hochberg, J. E. (1950). Figure-ground reversal as a function of visual satiation. *J Exp Psychol*, *40*, 682–6.
- Hock, H. S., Kelso, J. A. S., & Schöner, G. (1993). Bistability and hysteresis in the organization of apparent motion patterns. *J Exp Psychol Hum Percept Perform*, *19*, 63–80.
- Hock, H. S., Schöner, G., & Giese, M. (2003). The dynamical foundations of motion pattern formation: stability, selective adaptation, and perceptual continuity. *Percept & Psychophys*, *65*(2), 429–457.
- Hock, H. S., Schöner, G., & Hochstein, S. (1996). Perceptual stability and the selective adaptation of perceived and unperceived motion directions. *Vision Res*, *36*, 3311–3323.
- Hock, H. S., Schöner, G., & Voss, A. (1997). The influence of adaptation and stochastic fluctuations on spontaneous perceptual changes for bistable stimuli. *Percept & Psychophys*, *59*, 509–522.
- Hupé, J. M., & Rubin, N. (2003). The dynamics of bi-stable alternation in ambiguous motion displays: a fresh look at plaids. *Vis Res*, *43*, 531–548.
- Ittelson, W. H. (1952). *The Ames demonstrations in perception*. Princeton: Princeton University Press.
- Julesz, B., & Chang, J. J. (1976). Interaction between pools of binocular disparity detectors tuned to different disparities. *Biol Cybern*, *22*, 107–19.
- Kanizsa, G., & Luccio, R. (1995). Multistability as a research tool in experimental phenomenology. In P. Kruse & M. Stadler (Eds.), *Ambiguity in mind and nature* (pp. 47–68). Berlin: Springer.
- Köhler, W., & Wallach, H. (1944). Figural aftereffects; an investigation of visual processes. *Proc Amer Phil Soc*, *88*, 269–357.
- Kowler, E., & Anton, S. (1987). Reading twisted text—implications for the role of saccades. *Vis Res*, *27*, 45–60.
- Kruse, P., & Stadler, M. (Eds.). (1995). *Ambiguity in mind and nature*. Berlin: Springer.

² For other views on why vision might “shake up” the organization of the input, and allow for solutions that are not favored by stimulation, see Carpenter (1999) and Leopold and Logothetis (1999).

- Kruse, P., Stadler, M., & Wehner, T. (1986). Direction and frequency specific processing in the perception of long-range apparent movement. *Vision Res*, *26*, 327–35.
- Kubovy, M. (1994). The perceptual organization of dot lattices. *Psychon Bull Rev*, *1*(2), 182–190.
- Kubovy, M., Cohen, D. J., & Hollier, J. (1999). Feature integration that routinely occurs without focal attention. *Psychon Bull Rev*, *6*, 183–203.
- Kubovy, M., Holcombe, A. O., & Wagemans, J. (1998). On the lawfulness of grouping by proximity. *Cognit Psychol*, *35*, 71–98.
- Kubovy, M., & Wagemans, J. (1995). Grouping by proximity and multistability in dot lattices: A quantitative gestalt theory. *Psychol Sci*, *6*, 225–234.
- Landy, M. S., & Kojima, H. (2001). Ideal cue combination for localizing texture-defined edges. *J Opt Soc Am A*, *18*, 2307–2320.
- Leopold, D. A., & Logothetis, N. K. (1999). Multistable phenomena: changing views in perception. *Trends Cognit Sci*, *3*, 254–264.
- Marr, D. (1982). *Vision*. New York: Freeman.
- Rock, I. (1975). *Introduction to perception*. New York: Macmillan Publishing.
- Schiller, P. von. (1933). Stroboskopische Alternativversuche. *Psychologische Forschung*, *17*, 179–214.
- Triesch, J., Ballard, D. H., & Jacobs, R. A. (2002). Fast temporal dynamics of visual cue integration. *Perception*, *31*, 421–434.
- Williams, D., Phillips, G., & Sekuler, R. (1986). Hysteresis in the perception of motion direction as evidence for neural cooperativity. *Nature*, *324*, 253–255.